Mechanism and Interpolated Variational Transition State Rate Constant for the Reaction of Atomic H with Monoethylsilane†

Qingzhu Zhang, Yueshu Gu,* and Shaokun Wang

School of Chemistry and Chemical Engineering, Shandong University, Jinan 250100, P. R. China

Received: January 7, 2003; In Final Form: June 3, 2003

The reaction of atomic H and $EtSiH_3$ ($CH_3CH_2SiH_3$) has been studied theoretically by ab initio direct dynamics methods for the first time. This reaction involves three channels: H abstraction from the silicyl group (SiH_3), H abstraction from the methylene group (CH_2), and H abstraction from the methyl group (CH_3). At the QCISD(T)/6-311+G(3df,2p)//MP2/6-311G(2d,p) level, H abstraction from the silicyl group has the smallest potential barrier (4.58 kcal/mol). The potential barriers of H abstraction from the methylene and methyl groups are higher by 4−6 kcal/mol than that of H abstraction from the silicyl group. Changes of geometries, generalized normal-mode vibrational frequencies, and potential energies along the reaction paths for all the channels are discussed and compared. On the basis of the ab initio data, the rate constants of each channel have been deduced by canonical variational transition state theory (CVT) with a small-curvature tunneling (SCT) correction method over a wide temperatures range of 200−3000 K. The theoretical result has been compared with available experimental data. The kinetics calculations show that the variational effect is small, and in the low-temperature range (200−500 K), the small curvature tunneling effect is important for all the channels. The detailed branching ratios have been discussed.

1. Introduction

Alkylsilanes are common precursors used in chemical vapor deposition (CVD) to produce semiconductor devices. The gas-phase reactions of alkylsilanes with various atoms and free radicals have been the active subject of many studies for a long time.[1−13] In this paper we present a theoretical study on the reaction of atomic H with monoethylsilane $EtSiH_3$. The reasons for initiating such a work are 3-fold. First, the reaction with atomic hydrogen, the simplest free-radical species, is of particular interest: kinetics parameters for the H-atom reaction are desirable not only to provide an uncomplicated probe of chemical reactivity but also to throw light on the mechanism of the CVD processes. Second, the reaction mechanism has not been well characterized. Austin[2] suggested the predominant channel of this reaction is the abstraction of a hydrogen atom bound to silicon. Third, the effect of the replacement of H by an alkyl group on the strength and reactivity of the Si−H bond in SiH_4 is an interesting topic. Yu[9] studied systematically the reactions of H with $(CH_3)_{3-n}SiH_n$ ($n = 1-3$) and drew the conclusion that methyl substitution increases the reactivity of the Si−H bond. From the measured experimental rate constants, Austin came to a similar conclusion, that ethyl substitution increases the reactivity of the Si−H bond in SiH_4, and the rate constant with the same number of Si−H bonds is not changed noticeably when CH_3 is replaced by C_2H_5. Austin's conclusions need to be investigated and interpreted theoretically.

Only one experimental study is on record for the reaction of atomic H with $EtSiH_3$. Austin and Lampe[2] measured the relative rate constant in competitive experiments at 305 K in a static system, in which H atoms were produced by Hg-sensitized photolysis of H_2, and the rate of loss of $EtSiH_3$ was compared with that of C_2H_4 by means of time-of-flight mass spectrometry. To the best of our knowledge, little theoretical attention has been paid to this reaction. In this paper, we have initiated an exhaustive theoretical study of the application of ab initio electronic calculations combined with the variational transition-state theory for the reaction of atomic H with $EtSiH_3$. First, we have examined the reaction mechanism at high levels of ab initio molecular orbital theory. In a second step, we have carried out the kinetic calculation for this reaction. The calculated result was compared with the available experimental data.

2. Computational Methods

Using the Gaussian 98 programs,[14] high-level ab initio calculations have been carried out for the reaction of atomic H with $EtSiH_3$. The geometries of all the stationary points [the reactant, saddle points, and products] have been optimized at the unrestricted second-order perturbation Møller−Plesset level of theory (MP2) using the standard 6-311G(2d,p) basis set. Since unrestricted Hartree−Fock (UHF) reference wave functions are not spin eigenfunctions for open-shell species, we monitored the expectation values of $\langle S^2 \rangle$ in the MP2 optimization. The values of $\langle S^2 \rangle$ are always in the range 0.750−0.787 for doublets. After spin annihilation, the values of $\langle S^2 \rangle$ are 0.750, where 0.750 is the exact values for a pure doublet. Thus, spin contamination is not severe in the MP2/6-311G(2d,p) optimization. The harmonic vibrational frequencies have been calculated at the same level in order to determine the nature of the stationary points, the zero-point energy (ZPE), and the thermal contributions to the free energy of activation. Each saddle point was verified to connect the designated reactants and products by performing an intrinsic reaction coordinate (IRC) analysis. At the MP2/6-311G(2d,p) level, the minimum energy paths (MEP) were constructed for all channels independently, starting from the respective saddle point geometry and going downhill to both the asymptotic reactant and product channel with a gradient step

† Part of the special issue "A. C. Albrecht Memorial Issue".

* Corresponding author. E-mail: guojz@icm.sdu.edu.cn. Fax: 0531-8564464.

10.1021/jp030063e CCC: $25.00
Published on Web 07/24/2003

size of 0.02 amu$^{1/2}$ bohr. Along these MEPs the reaction coordinate, *s*, is defined as the signed distance from the saddle point, with $s > 0$ referring to the product side. In addition, for 30 points near the saddle point along the MEP, 15 points in the reactant side and 15 points in the product side, we computed the gradients and Hessians at the MP2/6-311G(2d,p) level, avoiding all the time-undesirable reorientations of molecular geometries.

Although the geometrical parameters and the frequencies of various species can be determined satisfactorily at the MP2/6-311G(2d,p) level (see *Geometry and Frequency*), the energies obtained at this level may not be accurate enough for the subsequent kinetics calculation. Therefore, a higher level, QCISD(T), and a more flexible basis set, 6-311+G(3df,2p), were employed to calculate the energies of various species.

The initial information obtained from our ab initio calculations allowed us to calculate the canonical variational rate constants including the tunneling effect. Canonical variational transition state theory (CVT)[15−17] is based on the idea of varying the dividing surface along a reference path to minimize the rate constant. The CVT rate constant for temperature *T* is given

$$k^{\mathrm{CVT}}(T) = \min_{s} k^{\mathrm{GT}}(T,s) \tag{1}$$

Where

$$k^{\mathrm{GT}}(T,s) = \frac{\sigma k_{\mathrm{B}} T Q^{\mathrm{GT}}(T,s)}{h \quad \Phi^{R}(T)} e^{-V_{\mathrm{MEP}}(s)/k_{\mathrm{B}}T} \tag{2}$$

Where, $k^{\mathrm{GT}}(T,s)$ is the generalized transition state theory rate constant at the dividing surface *s*, σ is the symmetry factor accounting for the possibility of more than one symmetry-related reaction path, k_{B} is Boltzmann's constant, *h* is Planck's constant, $\Phi^{\mathrm{R}}(T)$ is the reactant partition function per unit volume, excluding symmetry numbers for rotation, and $Q^{\mathrm{GT}}(T,s)$ is the partition function of a generalized transition state at *s* with a local zero of energy at $V_{\mathrm{MEP}}(s)$ and with all rotational symmetry numbers set to unity. All the kinetics calculations have been carried out with the POLYRATE 7.8[18] program. The rotational partition functions were calculated classically, and the vibrational modes were treated as quantum-mechanical separable harmonic oscillators. Finally, we considered the tunneling effect correction. Since the heavy−light−heavy mass combination is not present in the title reaction, the tunneling correction is calculated using the centrifugal-dominant small-curvature tunneling approximation (SCT).[19]

3. Result and Discussion

The optimized geometries of the reactant, saddle points, and products are shown in Figure 1. The saddle point of H abstraction from the silicyl group (SiH_3) is denoted as TS_1, while the saddle points of H abstraction from methylene (CH_2) and methyl groups (CH_3) are denoted as TS_2 and TS_3. The vibrational frequencies of the reactant, products, and saddle points are listed in Tables 1 and 2. The potential barriers ΔE, the reaction enthalpies ΔH, and the Si−H bond dissociation energies in $EtSiH_3$ calculated at various levels are summarized in Table 3. Figure 2 shows the classical potential energy (V_{MEP}) and vibrationally adiabatic potential energy ($V_{\mathrm{a}}^{\mathrm{G}}$) curves as functions of distance along the reaction coordinate *s* at the QCISD(T)/6-311+G(3df,2p)//MP2/6-311G(2d,p) level for all the channels. Change curves of generalized normal-mode vibrational frequencies with the reaction coordinate *s* are shown in Figure 3 for the channel of H abstraction from silicyl group (SiH_3). The calculated TST, CVT, and CVT/SCT rate constants are presented in Figure 4 a−c over the temperature range of 200−3000 K for all the channels. The CVT/SCT rate constants and the branching ratios are summarized in Table 4 for all the channels.

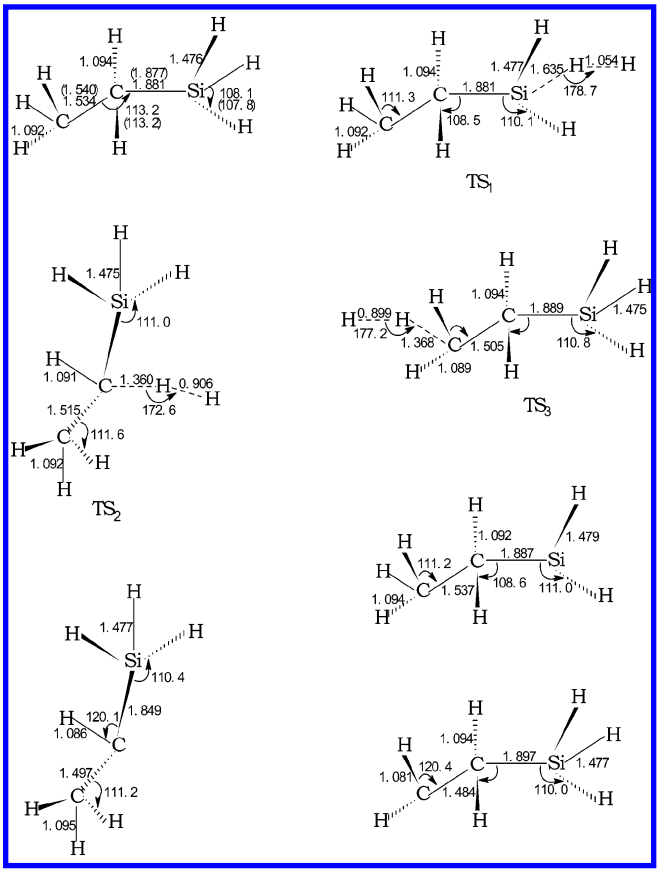

Figure 1. MP2/6-311G(2d,p) optimized geometries for stationary points. Distances are in angstroms, and angles are in degrees. The values in parentheses are the experimental data.[20]

TABLE 1: Harmonic Vibrational Frequencies (in cm^{-1}) for the Reactant and Products Involved in the Reaction of Atomic H with $EtSiH_3$ at the MP2/6-311G(2d,p) Level[a]

species	frequencies
$C_2H_5SiH_3$	3148, 3146, 3119, 3072, 3065, 2303, 2300(2163), 2298(2158), 1540, 1533, 1478, 1439, 1280, 1280, 1059, 1009, 994, 989, 985, 973, 780, 712, 616, 527, 234, 225, 144
$C_2H_5SiH_2$	3153, 3143, 3125, 3077, 3064, 2288, 2271, 1536, 1531, 1476, 1434, 1280, 1271, 1043, 1012, 987, 958, 777, 716, 657, 530, 240, 231, 152
CH_3CHSiH_3	3197, 3143, 3098, 3039, 2313, 2293, 2278, 1522, 1510, 1428, 1324, 1129, 1008, 998, 992, 981, 970, 734, 660, 636, 478, 238, 92, 28
$CH_2CH_2SiH_3$	3308, 3197, 3130, 3070, 2312, 2311, 2297, 1511, 1469, 1270, 1168, 1086, 987, 984, 981, 968, 774, 727, 605, 530, 479, 220, 214, 172

[a] The values in parenthesis are the experimental data.[21]

3.1. Reaction Mechanism. *a. Geometry and Frequency.* To clarify the general reliability of the theoretical calculations, it is useful to compare the predicated chemical properties with experimental data. As shown in Figure 1 and Table 1, the geometric parameters and harmonic vibrational frequencies of $EtSiH_3$ are in good agreement with the available experimental

TABLE 2: Harmonic Vibrational Frequencies (in cm^{-1}) for the Saddle Points Involved in the Reaction of Atomic H with $EtSiH_3$ at the MP2/6-311G(2d,p) Level

species	frequencies
TS_1	3151, 3145, 3121, 3073, 3065, 2297, 2287, 1539, 1532, 1476, 1437, 1280, 1277, 1125, 1059, 1028, 1010, 1005, 991, 965, 780, 735, 659, 535, 313, 259, 221, 151, 92,[a] 1633i
TS_2	3150, 3135, 3127, 3055, 2313, 2306, 2289, 1712, 1528, 1520, 1433, 1301, 1215, 1181, 1074, 1024, 993, 987, 979, 967, 808, 713, 639, 615, 317, 277, 228, 184, 116,[a] 1724i
TS_3	3211, 3127, 3122, 3071, 2308, 2308, 2302, 1784, 1496, 1473, 1291, 1223, 1222, 1209, 1065, 1007, 996, 985, 983, 969, 788, 729, 612, 572, 523, 318, 201, 159, 129,[a] 1716i

[a] The lowest-frequency vibrations of the transition states are considered as internal rotations.

values. From this result, it might be inferred that the same accuracy could be expected for other species. These good agreements give us confidence that the MP2/6-311G(2d,p) theory level is adequate to optimize the geometries and calculate the frequencies.

As mentioned above, three primary processes have been identified in the reaction of atomic H with $EtSi_2H_3$:

$$CH_3CH_2SiH_3 + H \rightarrow CH_3CH_2SiH_2 + H_2$$

H abstraction from SiH_3 group

$$CH_3CH_2SiH_3 + H \rightarrow CH_3CHSiH_3 + H_2$$

H abstraction from CH_2 group

$$CH_3CH_2SiH_3 + H \rightarrow CH_2CH_2SiH_3 + H_2$$

H abstraction from CH_3 group

The saddle point, namely, TS_1 in Figure 1, is located for the H abstraction from the silicyl group (SiH_3). The incoming H atom attacks one H of the silicyl group with a slightly bent orientation angle of 178.7°. At the MP2/6-311G(2d,p) level, the forming H−H bond of 1.054 Å is 42.82% longer than the equilibrium value of 0.738 Å in H_2, while the breaking Si−H bond is stretched by 10.77%. The saddle point TS_1 is reactant-like. Therefore, the channel of H abstraction from the silicyl group will proceed via an early saddle point. This rather early character in the saddle point TS_1 is in accordance with the low potential barrier and the high exothermicity of this channel, in keeping with Hammond's postulate.[22] The saddle point TS_1 has C_s symmetry.

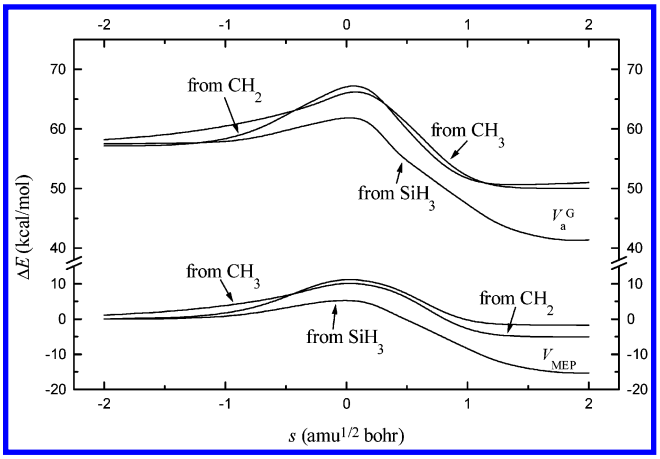

Figure 2. Classical potential energy (V_{MEP}) and vibrationally adiabatic potential energy (V_a^G) curves as functions of s at the QCISD(T)/6-311+G(3df,2p)//MP2/6-311G(2d,p) level for all the channels.

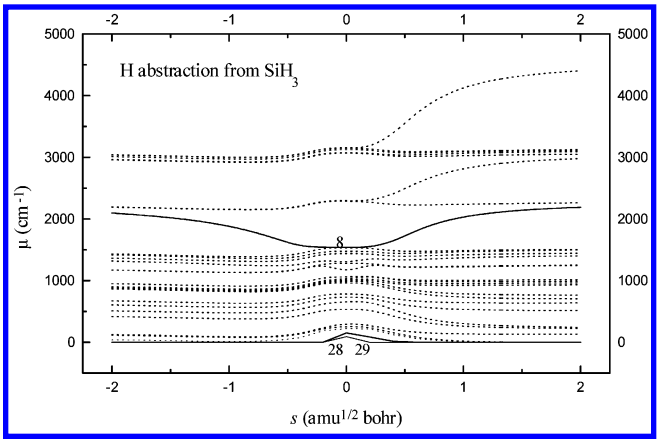

Figure 3. Changes of the generalized normal-mode harmonic vibrational frequencies as functions of s at the MP2/6-311G(2d,p) level for the channel of H abstraction from the silicyl group.

There are two channels for H abstraction from the ethyl group: H abstraction from the methylene group (CH_2) and H abstraction from the methyl group (CH_3), whose saddle points are denoted as TS_2 and TS_3. For the saddle points TS_2 and TS_3, the breaking C−H bonds are elongated by 24.31% and 22.76%, while the forming H−H bonds are longer than the equilibrium

TABLE 3: Potential Barriers ΔE (in kcal/mol), the Reaction Enthalpies ΔH (in kcal/mol), and the Si−H Bond Dissociation Energies in $EtSiH_3$ Calculated at Various Levels for All the Channels Involved in the Reaction of Atomic H with $EtSiH_3$[a]

Levels	ΔE_1	ΔE_2	ΔE_3	ΔH_1	ΔH_2	ΔH_3	D_0(Si-H)
MP2/STO-3G	35.54	38.08	38.79	11.73	18.81	16.38	108.51
MP2/3-21G	11.89	19.98	20.80	−12.70	2.35	3.50	17.15
MP2/6-31G	10.16	18.79	19.49	−15.00	−0.53	0.80	70.87
MP2/6-311G	8.55	17.23	17.97	−14.29	−1.06	−0.28	71.69
MP2/6-311G(d)	11.43	19.07	20.09	−7.85	2.19	3.96	78.13
MP2/6-311G(d,p)	8.55	14.07	14.97	−10.21	−1.72	−0.26	84.80
MP2/6-311G(2d,p)	8.94	14.39	15.24	−9.98	−1.65	0.00	85.03
MP2/6-311G(3df,2p)	7.96	13.81	14.72	−10.51	−2.09	−0.53	86.06
MP2/6-311+G(3df,2p)	7.85	13.77	14.66	−12.38	−2.22	−1.74	86.04
QCISD(T)/STO-3G	32.22	34.33	35.23	9.87	10.85	13.75	96.55
QCISD(T)/3-21G	9.59	16.17	17.15	−15.25	−2.02	−0.42	71.87
QCISD(T)/6-31G	7.77	15.50	15.75	−17.55	−5.08	−3.31	72.05
QCISD(T)/6-311G	5.72	13.71	13.98	−16.97	−5.53	−4.29	73.76
QCISD(T)/ 6-311G(d)	8.49	15.34	15.97	−10.81	−2.81	−0.25	79.92
QCISD(T)/6-311+G(3df,2p)	4.58	8.86	9.95	−15.68	−7.35	−4.50	88.36
exptl[24]							90.3 ± 1.2

[a] ΔE_1, ΔE_2, and ΔE_3 are the potential barriers of the channels of H abstraction from SiH_3, CH_2 and CH_3, respectively. ΔH_1, ΔH_2, and ΔH_3 are the reaction enthalpies of the channels of H abstraction from SiH_3, CH_2, and CH_3, respectively.

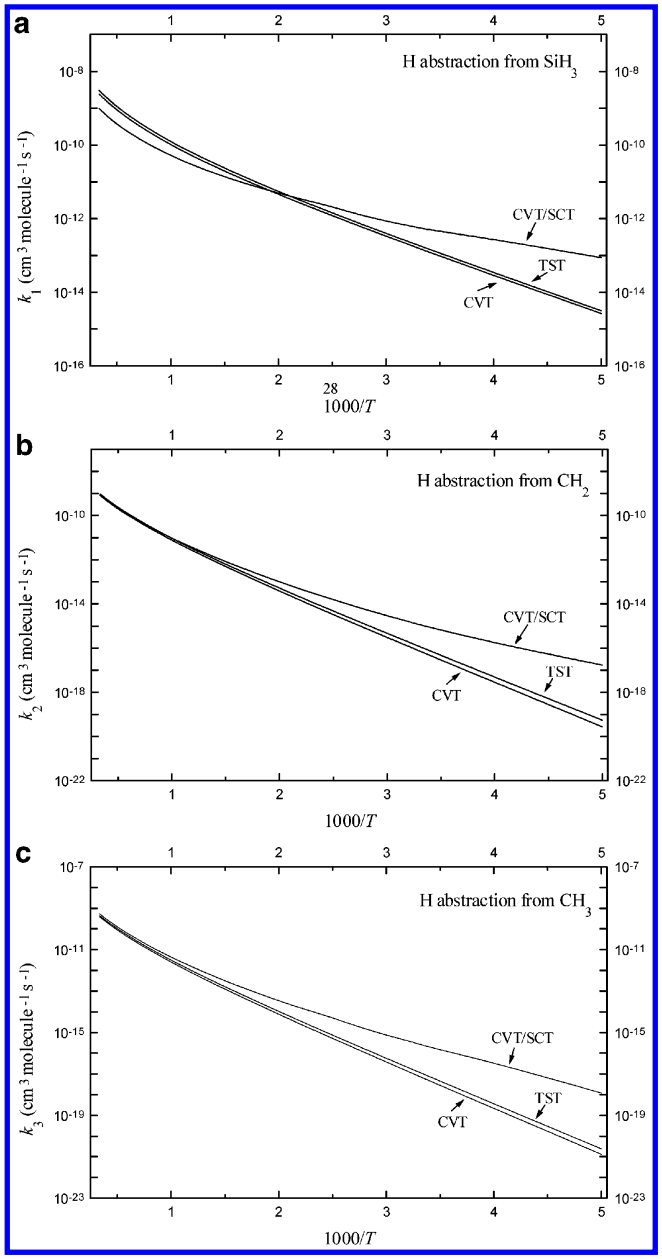

Figure 4. Rate constants as a function of the reciprocal of the temperature (T) in the temperature range of 200−3000 K for the all the channels.

value of 0.738 Å in H_2 by 22.76% and 21.82%, respectively. This indicates that both barriers of H abstraction from the ethyl group are almost centrally located.

Each saddle point was identified by one negative eigenvalue of the Hessian matrix and, therefore, one imaginary frequency. Since the imaginary frequency governs the width of the classical potential barrier along the MEP, it plays an important role in the tunneling calculations, especially when the imaginary frequency is large, and the associated eigenvector has a large component of hydrogenic motion. For saddle points TS_1, TS_2, and TS_3, the imaginary frequencies are 1633i, 1724i, and 1716i, so we expect that the tunneling effect should be important for the calculation of the rate constant. The modes of the lowest frequency are hindered internal rotation instead of small-amplitude vibration in TS_1, TS_2, and TS_3. The mode was removed from the vibrational partition function for the transition state and the corresponding hindered rotor partition function $Q_{HR}(T)$, calculated by the method devised by Truhlar,[23] was included in the expression for the rate constant.

To further confirm that these saddle points connect the designated reactants and products, the intrinsic reaction coordinate (IRC) has been calculated at the MP2/6-311G(2d,p) level from the saddle point to the reactants and the products. For the channel of H abstraction from the SiH_3 group, the breaking Si−H bond remains insensitive up to $s = -0.5$ amu$^{1/2}$ bohr and then increases smoothly. Meanwhile, the forming H−H bond shortens rapidly from reactants and reaches the equilibrium bond length in H_2 at $s = 0.5$ amu$^{1/2}$ bohr. Other bond lengths are almost unchanged during the reaction process. Therefore, the geometric change mainly takes place in the region from $s = -0.5$ to 0.5 amu$^{1/2}$ bohr. For the channels of H abstraction from CH_2 and CH_3 groups, the profiles of the changing of the bond lengths along the reaction paths are very similar. The breaking C−H bond and the forming H−H bond change strongly in the range $s = -0.5$ to 0.5 amu$^{1/2}$ bohr, and the other bond lengths are almost unchanged during the reaction process.

b. Energy. To choose a reliable theory level to calculate the energy, we calculated the Si−H bond dissociation energy in $EtSiH_3$ at various levels. On the basis of the similar Si−H bond strengths in SiH_4 and $EtSiH_3$, Luo and Pacey[24] estimated that the experimental dissociation energy of the Si−H bond in $EtSiH_3$ is 90.3 ± 1.2 kcal/mol at 0 K. The experiments give the spectrum dissociation energy, and so the calculated dissociation energies have been corrected for the ZPE. As seen from Table 3, the calculated results of D_0(Si−H) at the QCISD(T)/6-311+G(3df,2p) level are in good agreement with this experimental values. Therefore, the QCISD(T)/ 6-311+G(3df,2p) level is a good choice to calculate accurate energies for the title system.

Table 3 summarizes the calculated barrier heights ΔE and reaction enthalpies ΔH at various levels for each channel involved in the reaction of H with $EtSiH_3$. With respect to the potential barrier, the values obtained at the MP2 and QCISD(T) levels have a great discrepancy for the same channel. The effect of basis set on the potential barrier can be observed from our MP2 result with several different basis sets. From a basis with a Gaussian representation Slater-type orbitals (STO-3G) to Gaussian basis sets of double-ζ and triple-ζ (with both polarization and diffuse functions) quality, the barrier heights decrease drastically. The barrier heights decrease with the increase in polarization function at the MP2 level, while the barrier heights are almost unchanged with the increase in diffuse function (6-311G(3df,2p) → 6-311+G(3df,2p)). At the same basis set, as we raise the calculation levels (MP2 → QCISD(T)), the barrier height is lowered drastically.

Because of the absence of experimental standard heats of formation for the present reaction system, it is difficult to make a conclusive comparison of the reaction enthalpy. As seen from Table 3, the theory level and basis set have an important effect on the reaction enthalpy. Taking into account the calculated results of the Si−H bond dissociation energy in $EtSiH_3$, we think the QCISD(T)/ 6-311+G(3df,2p) level is the most reliable level. Therefore, in this paper, we choose the energies calculated at the QCISD(T)/6-311+G(3df,2p) level for the following kinetics calculation. At the QCISD(T)/6-311+G(3df,2p)//MP2/6-311G(2d,p) level, the channel of H abstraction from the SiH_3 group has the smallest potential barrier of 4.58 kcal/mol. The barrier heights of H abstraction from CH_2 and CH_3 groups are 4.28 and 5.37 kcal/mol higher than that of H abstraction from the SiH_3 group. This means that H abstraction from the SiH_3 group will be the dominant channel.

3.2. Kinetics Calculation. *a. Reaction Path Properties.* The minimum energy path (MEP) was calculated at the MP2/

TABLE 4: CVT/SCT Rate Constants and the Branching Ratios for All the Channels Involved in the Reaction of Atomic H with $EtSiH_3$ over the Temperature Range 200−3000 K (cm^3 $molecule^{-1}$ s^{-1})

T, K	k_1	k_2	k_3	k	k_1/k	k_2/k	k_3/k
200	8.79×10^{-14}	1.70×10^{-17}	1.19×10^{-18}	8.80×10^{-14}	1.00	0.00	0.00
250	2.78×10^{-13}	1.66×10^{-16}	3.55×10^{-17}	2.78×10^{-13}	1.00	0.00	0.00
298	5.24×10^{-13}	9.74×10^{-16}	2.20×10^{-16}	5.25×10^{-13}	1.00	0.00	0.00
305	5.90×10^{-13}	1.23×10^{-15}	3.12×10^{-16}	5.91×10^{-13}	1.00	0.00	0.00
350	1.04×10^{-12}	4.57×10^{-15}	1.15×10^{-15}	1.04×10^{-12}	1.00	0.00	0.00
400	2.11×10^{-12}	1.54×10^{-14}	5.22×10^{-15}	2.13×10^{-12}	0.99	0.01	0.00
450	3.33×10^{-12}	4.23×10^{-14}	1.41×10^{-14}	3.38×10^{-12}	0.99	0.01	0.00
500	4.94×10^{-12}	9.96×10^{-14}	3.37×10^{-14}	5.07×10^{-12}	0.97	0.02	0.01
600	9.48×10^{-12}	3.92×10^{-13}	1.42×10^{-13}	1.00×10^{-11}	0.95	0.04	0.01
700	1.61×10^{-11}	1.13×10^{-12}	4.38×10^{-13}	1.77×10^{-11}	0.91	0.06	0.02
800	2.52×10^{-11}	2.62×10^{-12}	1.09×10^{-12}	2.90×10^{-11}	0.87	0.09	0.04
900	3.70×10^{-11}	5.25×10^{-12}	2.30×10^{-12}	4.46×10^{-11}	0.83	0.12	0.05
1000	5.18×10^{-11}	9.37×10^{-12}	4.33×10^{-12}	6.55×10^{-11}	0.79	0.14	0.07
1200	9.01×10^{-11}	2.38×10^{-11}	1.19×10^{-11}	1.26×10^{-10}	0.72	0.19	0.09
1400	1.41×10^{-10}	4.89×10^{-11}	2.60×10^{-11}	2.16×10^{-10}	0.65	0.23	0.12
1600	2.04×10^{-10}	8.68×10^{-11}	4.86×10^{-11}	3.40×10^{-10}	0.60	0.26	0.14
1800	2.80×10^{-10}	1.40×10^{-10}	8.12×10^{-11}	5.01×10^{-10}	0.56	0.28	0.16
2000	3.70×10^{-10}	2.08×10^{-10}	1.25×10^{-10}	7.04×10^{-10}	0.53	0.30	0.17
2200	4.68×10^{-10}	2.94×10^{-10}	1.82×10^{-10}	9.44×10^{-10}	0.50	0.31	0.19
2400	5.80×10^{-10}	3.98×10^{-10}	2.51×10^{-10}	1.23×10^{-9}	0.47	0.32	0.21
2600	7.05×10^{-10}	5.18×10^{-10}	3.35×10^{-10}	1.56×10^{-9}	0.45	0.33	0.22
2800	8.37×10^{-10}	6.57×10^{-10}	4.31×10^{-10}	1.92×10^{-9}	0.43	0.34	0.23
3000	9.82×10^{-10}	8.15×10^{-10}	5.42×10^{-10}	2.34×10^{-9}	0.42	0.35	0.23

6-311G(2d,p) level by the IRC definition, and the energies of the MEP were refined by the QCISD(T)//MP2 method. For all channels the maximum position of the classical potential energy V_{MEP} curve at the QCISD(T)//MP2 level corresponds to the saddle point structure at the MP2/ 6-311G(2d,p) level. Therefore, the shifting of the maximum position for the V_{MEP} curve caused by the computational technique is avoided (avoiding artificial variational effect).[25,26] The changes of the classical potential energy V_{MEP} and the ground-state vibrational adiabatic potential energy V_a^G with the reaction coordinate *s* are shown in Figure 2 for all the channels. The classical potential energy V_{MEP} curve has a narrow barrier for each channel. Therefore, it is expected that the tunneling effect plays an important role for the calculation of the rate constants. The maximum positions of V_a^G energy curves are 0.09, 0.02, and 0.07 $amu^{1/2}$ bohr at the QCISD(T)//MP2 level for H abstraction from SiH_3, CH_2, and CH_3. For the same channel, the V_{MEP} and V_a^G curves are similar in shape. It means that the zero-point energy, ZPE, which is the difference of V_a^G and V_{MEP}, will have little change with *s*. To analyze this behavior in greater details, we show the variation of the generalized normal modes vibrational frequencies in Figure 3 for the channel of H abstraction from the silicyl group.

In the negative limit of *s*, the frequencies are associated with the reactants, while in the positive limit of *s*, the frequencies are associated with the products. For the channel of H abstraction from the silicyl group, the vibrational mode 8 (reactive mode) that connects the frequency of Si−H stretching vibration in $EtSiH_3$ with the frequency of the H−H stretching vibration of H_2 drops dramatically from $s = -1.0$ to $s = 1.0$ $amu^{1/2}$ bohr. This behavior is known to be typical of hydrogen-transfer reactions.[27−29] If changes in other frequencies were small, this drop could cause a considerable fall in the zero-point energy near the saddle point. The two lowest harmonic vibrational frequencies (modes 28 and 29, transitional modes) along the reaction path correspond to the transformation of free rotations or free translations of the reactant limit into real vibrational motions in the global system. Their frequencies tend asymptotically to zero at the reactant and product limits and reach their maximum in the saddle point zone. Therefore, in the saddle point region, the behavior of these transitional modes compensates the fall in the zero-point energy curve caused by the reactive mode. As a result, the zero-point energy curve shows little change variation with *s* and the V_{MEP} and V_a^G curves are similar in shape. The same conclusion can be drawn from the channels of H abstraction from CH_2 and CH_3 groups.

b. Rate Constant. The canonical variational transition state theory (CVT) with a small curvature tunneling correction (SCT), which has been successfully performed for several analogous reactions,[30−33] is an effective method to calculate the rate constant. In this paper, we used this method to calculate the rate constants for all the channels involved in the reaction of atomic H with $EtSiH_3$ over a wide temperature range from 200 to 3000 K. The calculated CVT/SCT rate constants are shown in Figure 4. For the purpose of comparison, the conventional transition state theory (TST) rate constants and the variational transition state theory (CVT) rate constants without the tunneling correction are also shown in Figure 4. Several important features of the calculated rate constants are the following:

(1) For all the channels, the TST rate constants, and the CVT ones are almost the same over the whole studied temperature range, which enables us to conclude that the variational effect is small for the calculation of the rate constant.

(2) For the channel of H abstraction from SiH_3 group, in the temperature range of 200−400 K, the CVT rate constants are much smaller than that of CVT/SCT. For example, at 298 K, the CVT rate constant is 1.38×10^{-13} cm^3 $molecule^{-1}$ s^{-1}, while the CVT/SCT rate constant is 5.24×10^{-13} cm^3 $molecule^{-1}$ s^{-1}. The latter is 3.8 times larger than the former. When the temperature is higher than 700 K, the CVT/SCT rate constants are smaller than that of CVT. This means the small curvature tunneling correction plays an important role for the calculation of the rate constant when $T < 400$ K and $T > 700$ K.

For the channels of H abstraction from CH_2 and CH_3 groups, the CVT rate constants are much smaller than that of CVT/SCT in the temperature range 200−500 K. The difference between the CVT rate constant and the CVT/SCT rate constant decreases with the increase in temperature. When the temperature is higher than 750 K, the CVT/SCT rate constants are asymptotic to the rate constants of CVT, which means only in the lower temperature range the small curvature tunneling correction plays an important role for the calculation of the rate constant.

(3) To provide clear information about the branching ratio, we listed the CVT/SCT rate constants and the branching ratios of each channel in Table 4. The CVT/SCT rate constants of the channel of H abstraction from the SiH_3 group are noted as k_1, while the rate constants of H abstraction from CH_2 and CH_3 groups are noted as k_2 and k_3. The total rate constants are noted as k, $k = k_1 + k_2 + k_3$. The branching ratios of the channels of H abstraction from SiH_3, CH_2, and CH_3 groups are noted as k_1/k, k_2/k, and k_3/k, respectively.

Due to having the smallest potential barrier, H abstraction from the SiH_3 group is the fastest reaction channel over the whole temperature range. In the temperature range 200−600 K, the rate constants for attack on the ethyl group are so small as to be negligible, so the channel for H abstraction from the SiH_3 group is the sole channel. However, as the temperature increases, H abstraction from CH_2 group becomes a competitive reaction channel. When the temperature is higher than 1000 K, the rate constants of attack on the CH_2 group is more than 14% of the total values. Due to having the highest potential barrier, the contribution of H abstraction from the CH_3 group is minor over the whole studied temperature range. In the lower temperature range, the rate constant k_3 is so small that it can be considered to be negligible. When $T \geqslant 600$ K, the rate constant k_3 cannot be considered to be negligible and will account for some branching ratio to the overall rate constants. For example, at $T = 1000$ K, $k_3/k = 0.07$.

(4) At 305 K, the total CVT/SCT rate constant, which is the sum of the CVT/SCT rate constants for all the channels, is 5.91×10^{-13} cm^3 molecule^{-1} s^{-1}, which is in good agreement with the experimental value[2] of 7.5×10^{-13} cm^3 molecule^{-1} s^{-1}. Both the TST method and the CVT method without the tunneling effect correction underestimate rate constants. Therefore, the CVT/SCT rate constants are taken as the accurate rate constants for each channel.

(5) It is obvious that the calculated rate constants exhibit typical non-Arrhenius behavior. This non-Arrhenius behavior has frequently been observed in radical-molecule reactions studied over wide temperature ranges. All the CVT/SCT rate constants of the title reaction are fitted by a three-parameter formula over the temperature range 200−3000 K and given in units of cm^3 molecule^{-1} s^{-1} as follows:

$$k = (5.74 \times 10^{-20}) T^{3.08} \exp(-424.48/T)$$

(6) It is very interesting to compare the strength and reactivity of the Si−H bond in SiH_4, CH_3SiH_3, and $EtSiH_3$. Yu studied theoretically the reactions of H with SiH_4[2] and CH_3SiH_3.[2] At the G2//QCISD/6-311+G(d,p) level, the potential barrier of the reaction of H with SiH_4 is 5.54 kcal/mol. At the PMP4/6-311+G(3df,2p)//BHLYP/6-311+G(d,p) level, the potential barrier of H abstraction from the SiH_3 group in CH_3SiH_3 is 4.84 kcal/mol. To eliminate the error caused by the level of theory, we recalculated the potential barriers of H abstraction from the silicyl group in SiH_4 and CH_3SiH_3 at the QCISD(T)/6-311G(3df,2p)//MP2/6-311G(2d,p) level. The values are 5.79, 4.49, and 4.58 kcal/mol for H abstraction from the silicyl group in SiH_4, CH_3SiH_3, and $EtSiH_3$, respectively. The barrier heights for H abstraction from the silicyl group in CH_3SiH_3 and $EtSiH_3$ are 1.2−1.3 kcal/mol lower than that for H abstraction from SiH_4, which means that it is more difficult to abstract H from SiH_4 than from the silicyl group in CH_3SiH_3 and $EtSiH_3$. The effect of the replacement of H by methyl and ethyl groups on the reactivity of the Si−H bond can be seen by evaluating the room-temperature k/n, the room-temperature rate constant corrected for the reaction-path degeneracy, where n is the number of Si−H bonds. At 298 K, the k/n for the reaction of H with SiH_4 is 3.12×10^{-14} cm^3 molecule^{-1} s^{-1};[34] for H abstraction from the silicyl group in CH_3SiH_3[9] and $EtSiH_3$, the values of k/n are 1.28×10^{-13} and 1.75×10^{-13} cm^3 molecule^{-1} s^{-1}, respectively. The k/n values of H abstraction from the silicyl group in CH_3SiH_3 and $EtSiH_3$ are nearly identical. The k/n value of H abstraction from SiH_4 is slightly smaller than that of H abstraction from the silicyl group in CH_3SiH_3 and $EtSiH_3$. This verified Austin's view that the replacement of H by methyl and ethyl groups increases the reactivity of the Si−H bond in SiH_4, and the rate constants calculated for a species with the same number of Si−H bonds is not changed noticeably when CH_3 is replaced by C_2H_5.

4. Conclusion

In this paper, we studied the reaction of atomic H with $EtSiH_3$ using ab initio electronic structure theory and canonical variational transition state theory (CVT) with small-curvature tunneling (SCT) correction. The reaction mechanism and kinetic nature were reported over the temperature range 200−3000 K. Several major conclusions can be drawn from this calculation:

(1) At lower temperatures, hydrogen abstraction from the SiH_3 group is the sole channel. With increasing temperature, hydrogen abstractions from the CH_2 and CH_3 groups become the competitive channels.

(2) The variational effect is small for all the channels.

(3) The small curvature tunneling correction plays an important role for the calculation of the rate constants.

(4) At 305 K, the CVT/SCT overall rate constant is in good agreement with the experimental value. Both the TST method and the CVT method without tunneling underestimate the rate constants.

Acknowledgment. We thank Professor Donald G. Truhlar for providing the POLYRATE 7.8 program. This work is supported by the Research Fund for the Doctoral Program of Higher Education of China.

References and Notes

(1) Arthur, N. L.; Miles, L. A. *Chem. Phys. Lett.* **1998**, *282*, 192.
(2) Austin, E. R.; Lampe, F. W. *J. Phys. Chem.* **1977**, *81*, 1134.
(3) Arthur, N. L.; Potzinger, P.; Reimann, B.; Steenbergen, H. P. *J. Chem. Soc., Faraday Trans. 2* **1989**, *85*, 1447.
(4) Horie, O.; Taege, R.; Reimann, B.; Arthur, N. L.; Potzinger, P. *J. Phys. Chem.* **1991**, *95*, 4393.
(5) Misra, A.; Ding, L.; Marshall, P. *J. Phys. Chem.* **1994**, *98*, 4020.
(6) Worsdorfer, K. Ph.D. Thesis, Universithof Essen, Germany, 1978.
(7) Hoffmeyer, H.; Horie, O.; Potzinger, P.; Reimann, B. *J. Phys. Chem.* **1985**, *89*, 2901.
(8) Espinosa-Garcia, J.; Sanson, J.; Corchado, J. C. *J. Chem. Phys.* **1998**, *109*, 466.
(9) Yu, X.; Li, S.-M.; Xu, Z.-F.; Li, Z.-S.; Sun, C.-C. *J. Phys. Chem. A* **2001**, *105*, 7072.
(10) Ding, L.; Marshall, P. *J. Am. Chem. Soc.* **1992**, *114*, 5754.
(11) Ding, L.; Marshall, P. *J. Phys. Chem.* **1992**, *96*, 2197.
(12) Doncaster, A. M.; Walsh, R. *J. Chem. Soc., Faraday Trans.* **1979**, *75*, 1126.
(13) Arthur, N. L.; Bell, T. N. *Rev. Chem. Intermed.* **1978**, *2*, 37.
(14) Frisch, M. J.; Trucks, G. W.; Schlegel, H. B.; Gill, P. W. M.; Johnson, B. G.; Robb, M. A.; Cheeseman, J. R.; Keith, T. A.; Petersson, G. A.; Montgomery, J. A.; Raghavachari, K.; Allaham, M. A.; Zakrzewski, V. G.; Ortiz, J. V.; Foresman, J. B.; Cioslowski, J.; Stefanov, B. B.; Nanayakkara, A.; Challacombe, M.; Peng, C. Y.; Ayala, P. Y.; Chen, W.; Wong, M. W.; Andres, J.; Replogle, E. S.; Gomperts, R.; Martin, R. L.; Fox, D. J.; Binkley, J. S.; Defrees, D. J.; Baker, J.; Stewart, J. P.; Head-Gordon, M.; Gonzales, C.; Pople, J. A. *GAUSSIAN 98*, revision-A.7; Gaussian: Pittsburgh, PA, 1998.
(15) Gonzalez-Lafont, A.; Truong, T. N.; Truhlar, D. G. *J. Chem. Phys.* **1991**, *95*, 8875.
(16) Garrett, B. C.; Truhlar, D. G. *J. Phys. Chem.* **1979**, *83*, 1052.

(17) Garrett, B. C.; Truhlar, D. G.; Grev, R. S.; Magnuson, A. W. *J. Phys. Chem*. **1980**, *84*, 1730.
(18) Steckler, R.; Chuang, Y. Y.; Fast, P. L.; Corchade, J. C.; Coitino, E. L.; Hu, W. P.; Lynch, G. C.; Nguyen, K.; Jackells, C. F.; Gu, M. Z.; Rossi, I.; Clayton, S.; Melissas, V.; Garrett, B. C.; Isaacson, A. D.; Truhlar, D. G. *POLYRATE Version*; University of Minnesota: Minneapolis, 1997.
(19) Liu, Y.-P.; Lynch, G. C.; Truong, T. N.; Lu, D.-H.; Truhlar, D. G.; Garrett, B. C. *J. Am. Chem. Soc*. **1993**, *115*, 2408.
(20) Hayashi, M.; Matsumura, C. *Bull. Chem. Soc. Jpn*. **1972**, *45*, 732.
(21) McKean, D. C.; Morrisson, A. R.; Torto, I.; Kelly, M. I. *Spectrochim. Acta, Part A* **1985**, *41*, 25.
(22) Hammmond, G. S. *J. Am. Chem. Soc*. **1955**, *77*, 334.
(23) Truhlar, D. G. *J. Comput. Chem*. **1991**, *12*, 266.
(24) Luo, Y.-P.; Pacey, P. D. *Can. J. Chem*. **1993**, *71*, 572.
(25) Malick, D. K.; Petersson, G. A.; Montgomery, J. A., Jr. *J. Chem. Phys*. **1998**, *108*, 5704.
(26) Espinosa-Garcia, J.; Corchado, J. C. *J. Phys. Chem*. **1995**, *99*, 8613.
(27) Truhlar, D. G.; Isaacson, A. D. *J. Chem. Phys*. **1982**, *77*, 3516.
(28) Corchado, J. C.; Espinosa-Garcia, J. *J. Chem. Phys*. **1997**, *106*, 4013.
(29) Espinosa-Garcia, J.; Corchado, J. C. *J. Phys. Chem*. **1996**, *100*, 16561.
(30) Zhang, Q.-Z.; Gu, Y.-S.; Wang, S.-K. *J. Chem. Phys*. **2003**, *118*, 633.
(31) Zhang, Q.-Z.; Zhang, D.-J.; Wang, S.-W.; Gu, Y.-S. *J. Phys. Chem. A* **2002**, *106*, 122.
(32) Zhang, Q.-Z.; Wang, S.-K.; Gu, Y.-S. *J. Phys. Chem. A* **2002**, *106*, 3796.
(33) Zhang, Q.-Z.; Wang, S.-K.; Gu, Y.-S. *J. Phys. Chem. A* **2002**, *106*, 9071.
(34) Yu, X.; Li, S.-M.; Li, Z.-S.; Sun, C. C. *J. Phys. Chem. A* **2000**, *104*, 9207.